

H. PAUL\*, \*\*, J.H. DRIVER\*\*\*

**DEFORMATION BEHAVIOUR OF CHANNEL-DIE COMPRESSED Al BICRYSTALS  
WITH  $\{100\}<001>/\{110\}<011>$  ORIENTATION**

**UMOCNIENIOWE ZACHOWANIE SIĘ NIESWOBODNIE ŚCISKANYCH BIKRYSTAŁÓW Al  
O UKŁADZIE ORIENTACJI  $\{100\}<001>/\{110\}<011>$**

The formation of band-like heterogeneities in deformed grains and the evolution of their microtexture components during large plastic deformations is examined in Al bicrystals. The study has focussed on bands developed by plane strain compression in  $\{100\}<001>/\{110\}<011>$  (soft/hard)-oriented high purity aluminium bicrystals with the boundary plane situated parallel to the compression plane. The character of the bands was determined by systematic local orientation measurements using EBSD in SEM-FEG scanning electron microscope and also by transmission electron microscopy (TEM/CBED) at specific locations.

The bicrystal deformation analysis shows that the microtexture evolution in each crystallite is quite different. Very strong deformation banding in the 'cube' grain is initiated by strain incompatibilities and giving initial rotations about transverse direction. At very high strains where the flow is inhomogeneous, clearly defined rotations about a  $\langle 112 \rangle$  axis are observed, suggesting localized single  $\{111\}<110>$  slip in areas of the band. The 'hard'  $\{110\}<011>$ -oriented grains are more stable under plane strain conditions except for the zone near the grain boundary where strong micro-textural/structural disturbances are observed.

*Keywords:* Aluminium; Bicrystals; Microtexture; Deformation bands; SEM-FEG

W pracy analizowano problem formowania się pasmowych niejednorodności odkształcenia oraz ich wpływ na ewolucję mikrostruktury i tekstury stanu odkształconego. Analiza bazuje na pasmach formujących się w bikryształach aluminium o układzie orientacji ziaren  $\{100\}<001>/\{110\}<011>$ , z granicą pomiędzy krystalitami usytuowaną równolegle do płaszczyzny ściskania, poddanych nieswobodnemu ścisnaniu. Identyfikację mechanizmów odpowiedzialnych za obserwowane tendencje rota-

\* INSTYTUT METALURGII I INŻYNIERII MATERIALOWEJ IM. A. KRUPKOWSKIEGO PAN, 30-059 KRAKÓW, UL. REYMONTA 25

\*\* WYDZIAŁ MECHANICZNY, UNIwersytet ZIELONOGÓRSKI, 65-246 ZIELONA GÓRA, UL. PODGÓRNA 50

\*\*\* ECOLE NATIONALE SUPÉRIEURE DES MINES DE SAINT ETIENNE, CENTRE SMS, 158 COURS FAURIEL, 42023 SAINT ETIENNE CEDEX2, FRANCE, CNRS FEDERATION 2145 AND UMR 5146

cji sieci krystalicznej przeprowadzono z użyciem transmisyjnej (TEM) i skaningowej (SEM) mikroskopii elektronowej, wykorzystujących techniki pomiaru orientacji lokalnych.

Zachowanie umocnieniowe oraz ewolucja początkowej orientacji obydwu krystalitów formujących bikryształ są całkowicie odmienne. Ziarna o orientacji  $\{100\}\langle 001\rangle$  wykazują silną tendencję do formowania pasm odkształcenia. Z krystalograficznego punktu widzenia proces przejścia od orientacji osnowy do orientacji pasma, stowarzyszony jest z rotacją sieci krystalicznej dookoła osi  $\langle 112\rangle$  sugerującej aktywację pojedynczego poślizgu typu  $\{111\}\langle 110\rangle$ . Krystality o orientacji  $\{110\}\langle 110\rangle$ , w badanym zakresie deformacji są bardziej stabilne, za wyjątkiem obszarów bezpośrednio przylegających do granicy ziaren gdzie obserwowano wystąpienie silnych zaburzeń sieci krystalicznej.

## 1. Introduction

The formation of band-like deformation heterogeneities is a typical result of the plastic behaviour of many unstable crystallites in f.c.c. metals. However, earlier investigations have almost always concentrated on either polycrystal or single crystal specimens, often in relation to the role played by plastic instabilities in the processes of macroscopic deformation texture formation. There is, however, little information on texture evolution and the formation of different kinds of strain heterogeneities in bicrystals, where the grain boundary is strictly defined; some notable exceptions are given in references [1, 2]. The choice of bicrystals as a model material obviously enables one to study the role of the grain boundary in band propagation and texture transformation. It also avoids the major disadvantage of polycrystal deformation where the active surface of the grain boundaries drastically increases with increasing deformation. The aim of the present study is to examine the microtexture evolutions during the formation of plastic instabilities in an aluminium bicrystal containing grains with high symmetry orientations. The crystallites configuration has been chosen to simulate the behaviour of two extreme orientations: very 'soft' ( $\{100\}\langle 001\rangle$  with a Taylor factor of  $\sqrt{6}$ ) vs. very 'hard' ( $\{110\}\langle 011\rangle$  with a Taylor factor of  $2\sqrt{6}$ ).

The behaviour of the 'cube' grains in plane strain compression at  $T < 0.5T_f$  is particularly interesting since they are known to break up into highly mis-oriented deformation bands. The experimentally observed rotations, predominantly around the transverse direction (TD) [3-8], associated with band formation, differ from the earlier analyses of Dillamore and Kato [9], who predicted for rolled samples large rotations about the normal (ND) and the rolling (RD) directions, and of Lee and Duggan [10] who predicted large divergent lattice rotations about ND and TD. The application of modern TEM local orientation measurements and SEM/EBSD orientation mapping permits the analysis of the microtexture scattering both within and outside the deformation bands.

## 2. Materials and methods

Aluminium bicrystals with a selected pair of orientations denoted 'cube'  $\{100\}\langle 001 \rangle$ /'hard'  $\{110\}\langle 011 \rangle$  were the object of the present study. A high purity (99.998%) bar with controlled orientation was grown by a modified Bridgman technique (horizontal solidification), using a split graphite mould. The dimensions of the bicrystal bar were approximately 15 mm (thickness)  $\times$  22 mm (width)  $\times$  150 mm (length), with the grain boundary situated parallel to the compression plane. The samples were compressed in a channel-die at the initial strain rate of  $\sim 10^{-4}\text{s}^{-1}$ . To avoid the formation of "diffuse" deformation bands, as occurs at room temperature in Al, the tests were performed at 77K by immersing the channel-die device in a reservoir with liquid nitrogen for the duration of the tests. This procedure is designed to give, at relatively low strains, a work-hardened structure containing clearly defined bands. The majority of the metallographic observations were made on the longitudinal plane, i.e. ND-ED.

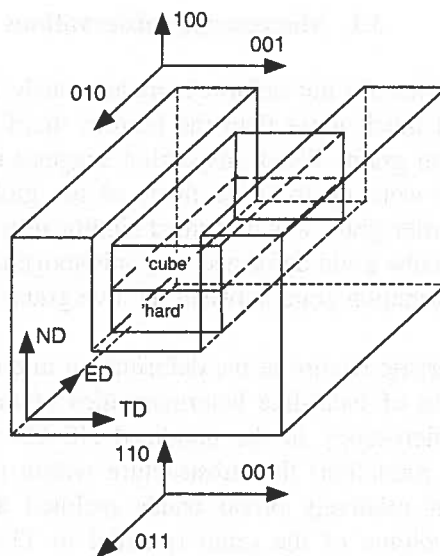


Fig. 1. The crystallographic directions within 'cube' and 'hard' grains and the situation of the grain boundary

The orientations of the crystallites forming the bicrystal before compression were checked by back reflexion Laue X-ray. The deformed specimens were mostly examined by scanning electron microscopy (SEM) in a JEOL JSM 6500F, equipped with a field emission gun (FEG) and electron backscattered diffraction (EBSD) facilities acquisition where microscope control pattern acquisition and solution were performed with the HKL Channel 5 system. The samples were also examined by TEM using a 200kV Philips TEM CM200 and convergent beam electron diffraction (CBED) with semi-automatic Kikuchi pattern analysis. Local orientation data, obtained by

TEM/CBED and SEM/EBSD techniques on the ND-ED or ND-TD planes, were usually transformed to the standard ED-TD reference system and presented in the form of {111} pole figures.

The situation of the bicrystal in the channel-die device and the nominal orientations of the grains are shown in Fig. 1. The configuration is such that bicrystal boundary plane is parallel to TD||<100>. The interrelation between the grain orientations forming a bicrystal, could be described by the relation:

$$\{110\}\langle 011\rangle \rightarrow 45^\circ \langle 100\rangle \parallel \text{TD}(\{100\}\langle 001\rangle)$$

which indicates that the crystallites possessed a common {100} plane, perpendicular to TD.

### 3. Results and discussion

#### 3.1. Macroscopic observations

The bicrystal samples did not deform homogeneously in the channel-die; the top 'cube' grain deformed much more than the bottom 'hard' grain and tended to flow out and over the bottom grain. Visual inspection suggests that the softer 'cube' grain underwent strains that were up to twice those of the global, or nominal, thickness reduction while the harder grain was deformed significantly less. Exact values are difficult to give since the cube grain deformed very inhomogeneously. It was also apparent that the transition deformation zone between the two grains was mostly situated in the 'hard' grain.

The most characteristic feature of the deformation microstructure of a {100}<001> crystal is the formation of band-like heterogeneities of deformation. The bands are revealed by optical microscopy in the anodized ND-ED plane. At lower deformations (<43% nominal reduction) the substructure within {100}<001>-oriented crystallite is composed of relatively broad bands inclined at ~35–45° to ED. They penetrate the whole volume of the grain (parallel to TD) and usually separate areas with large lattice rotations, but do not show any tendency to intersect the grain boundary. The process of band formation increases greatly with the deformation so that after 59% deformation they practically fill the whole volume of the crystallite.

#### 3.2. The development of deformed microtexture

*'Cube'-oriented crystallite.* The deformation bands are periodically distributed on the longitudinal plane, run across the whole volume of the crystal and show different inclinations with respect to ED. At relatively low strains most of the substructure is occupied by elongated areas, with a low density of misoriented sub-boundaries, and

separated by areas with a high density of dislocation sub-boundary arrays (Fig. 2a for 43% reduction). At this stage the bands are clearly rotated by about  $\pm 25^\circ$  around TD. Note that this rotation tends to bring the initial 'cube' grain closer to the 'hard' grain orientation ( $\pm 45^\circ$  around TD), Fig. 2b-d. The misorientation angle across the bands attains values within the range of  $35\text{-}40^\circ$  (Fig. 2e), and the misorientation axes were

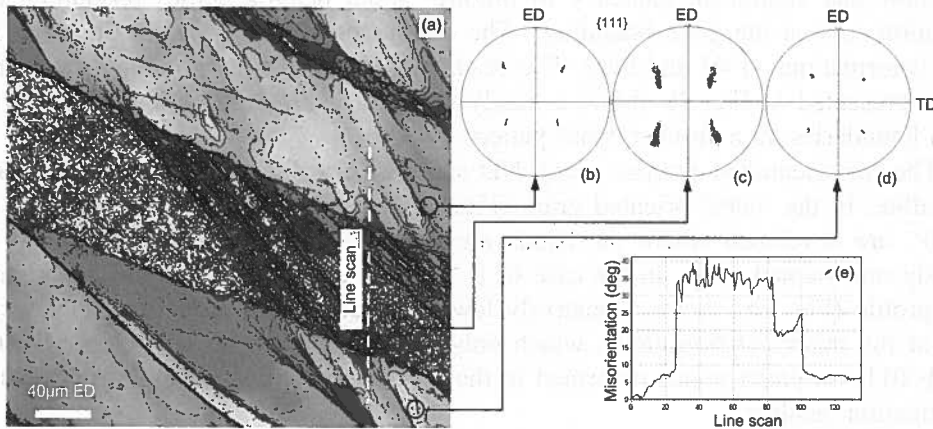


Fig. 2. (a) Kikuchi quality band contrast map from the area of 'cube'-oriented grain and (b)-(d) the corresponding  $\{111\}$  pole figures (e) Line scan across the elongated area with high dislocation density. SEM/EBSD local orientation measurements in the plane of ND-ED with step size of 200nm. Sample deformed 43%

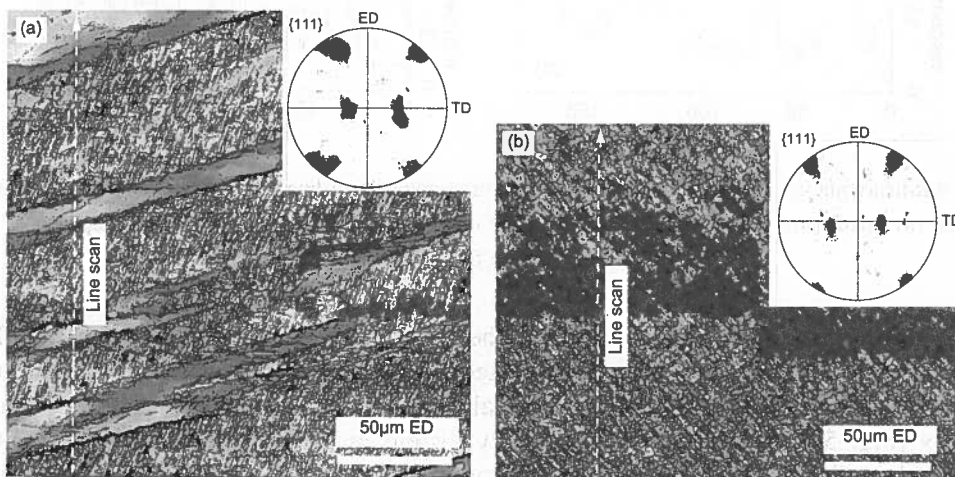


Fig. 3. Kikuchi band quality map from the areas of: (a) 'cube'-oriented grain and (b) middle part of a 'hard' crystallite and the corresponding  $\{111\}$  pole figures. SEM/EBSD measurements in ND-ED plane with step size of 200nm. Sample deformed 59%

then closer to a  $\langle 112 \rangle$  direction. At higher strains there are further lattice rotations associated with the gradual disappearance of the less misoriented volumes. After 59%

reduction the substructure is finer than that at 43% reduction, and the areas saturated by sub-grain boundaries tend to occupy a significant part of the 'cube' crystallite. An example of this microstructure, is presented in Fig. 3a as an Kikuchi band quality map, with marked grain boundaries of  $>1^\circ$  and  $>15^\circ$ .

*'Hard'-oriented crystallite.* For the deformations applied here, this crystallite does not show any significant tendency to produce strain heterogeneities (excluding the transition zone at the grain boundary). The orientation spread is nearly the same for both deformations of 43 and 59%. The orientation map from the middle layer of the grain, presented in Fig. 3b shows a nearly uniform distribution of low angle ( $>1^\circ$ ) grain boundaries, in a checker-board pattern.

The misorientation profiles along ND show a very different behaviour for each crystallite. In the 'cube'-oriented grain (Fig. 4a) strong misorientation angles, of up to  $30^\circ$ , are developed where the bands are crossed. These peaks are separated by slightly misoriented areas. In the case of a 'hard'-oriented crystallite the misorientation profile (Fig. 4b) shows a relatively low amplitude and a high frequency variation of the misorientation angle, which only sporadically attains  $10^\circ$ . Generally, the  $\{110\}<011>$ -oriented grains deformed to the maximum applied strain did not exhibit deformation banding.

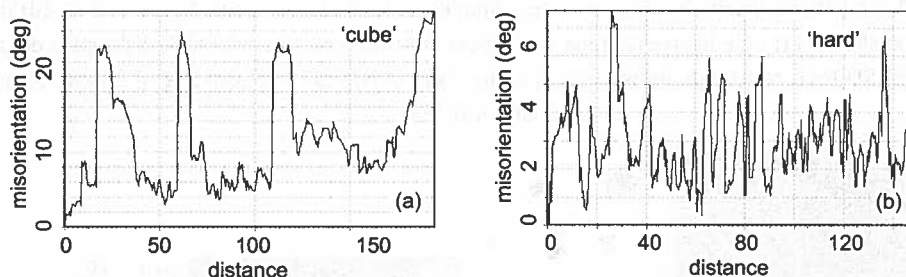


Fig. 4. Misorientation with respect to the first measured point along line scan parallel to ND. (a) 'cube' and (b) 'hard' parts of the bicrystal. SEM/EBSD measurements in ND-ED plane with step size of 200nm. Sample deformed 59%

*Region of the bicrystal boundary.* On the longitudinal plane before deformation the bicrystal boundary was a straight line situated along ED. However, during deformation, which induces strong changes of the crystallite shape, bending of the grain boundary occurs (Fig. 5a). This is especially clearly visible in the 'hard'-oriented crystallite, where the volumes lying near the boundary must accommodate the incompatibilities between the neighbouring grains. The existence of the boundary region indicates that this crystal does not rotate as a whole but splits up into different areas with a broad orientation spread. The  $\{111\}$  pole figure measured on the longitudinal plane, shown in Fig. 5b, contains the orientations from a large area of  $200\mu\text{m} \times 5000\mu\text{m}$  (longer axis along ED) across the grain boundary and the transition zone (near the free surfaces of the sample). It shows a strong, continuous dispersion of the  $<111>$  poles characterized

by strong scattering of the poles by (+/-)TD rotation with some additional rotations around ED and ND axes.

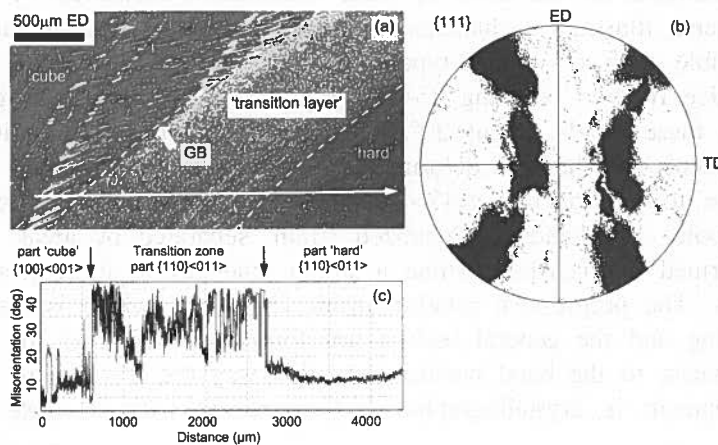


Fig. 5. (a) Microstructure of the transition zone near the grain boundary. (b)  $\{111\}$  pole figure showing orientation changes across the grain boundary and transition zone (scan area of  $200\mu\text{m} \times 5000\mu\text{m}$ ). (c) Misorientation profile with respect to the first point lying within the 'cube' grain across the transition zone. SEM/EBSD measurements in ND-ED plane with step size of 200nm.

Sample deformed 59%

The misorientations, calculated with respect to the first measured point lying within the 'cube' grain across the grain boundary, reflect the difference in the structure that is formed (Fig. 5c). There is only about  $12^{\circ}$ - $15^{\circ}$  between the 'hard' grain and the first measured point in the 'cube' grain as a result of the rapid rotation of the 'cube' grain near the transition zone towards the  $\{110\}\langle 011\rangle$  orientation). In the 'cube' crystallite the misorientation angle very often attains values of  $25$ - $35^{\circ}$ , resulting from the deformation bands. Across the transition region lying near the grain boundary there is a rapid increase and subsequent high amplitude changes of the misorientation angle. The regions remote from the boundary in the  $\{110\}\langle 011\rangle$ -oriented crystallite show a gradual disappearance of the orientation variation. A detailed analysis of the misorientation axes distribution has shown that they are close to the  $\langle 100 \rangle$  axis ( $\parallel$  TD). Additionally, misorientation axes in the range of the  $\langle 110 \rangle$ - $\langle 112 \rangle$  directions are observed.

### 3.3. Orientation changes as a result of deformation banding

TEM can provide information about some detailed features of the matrix — band interfaces as a result of quantitative measurements of individual cell orientations with dimensions down to tens of nanometers.

Fig. 6a shows a TEM microstructure observed along ED of a 'cube'-oriented crystallite after a thickness reduction of 59%; it is composed of regular lay-

ers of deformation bands separated by less dislocated matrix. The typical deformation bands observed here have widths in the range  $1\text{-}10\mu\text{m}$ . The  $\{111\}$  pole figures, constructed on the basis of local orientations measured by a line scan across the band, illustrate a characteristic tendency for the microtexture with usually one stable pole of  $\langle 111 \rangle$ -type (Figs. 6b and c). The band is associated with lattice rotation reaching  $35\text{-}40^\circ$  (Fig. 6d). The orientation gradients established in these bands, about  $20^\circ/\mu\text{m}$ , are very high for aluminium, perhaps as a consequence of the low deformation temperature. In this case the rotation axis is close to one of the  $\langle 112 \rangle$  directions, situated near the relatively stable  $\langle 111 \rangle$  pole. The bands of localized strain, separated by areas of relatively weakly deformed matrix, demonstrate a strong tendency to form groups of compact bundles. The progressive rotation inside the bands which is responsible for lattice bending and the general texture transformation, describes the lattice rotation from matrix to the band positions. In this way the mechanism of advanced band development is crystallographic and *connected with a single slip operation*.

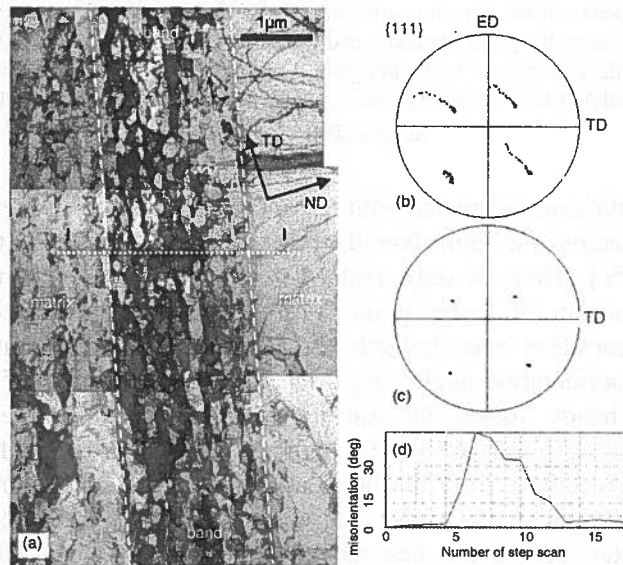


Fig. 6. (a) TEM microstructure of band-like strain inhomogeneties in a crystallite with 'cube' orientation, and the corresponding  $\{111\}$  pole figures obtained within (b) the band and (c) the matrix areas. (d) Misorientation along line scan with respect to the first measured point. TEM/CBED measurements. Sample deformed 59%

In earlier studies on single crystals, many authors interpreted the broad scattering of the initial crystal orientation as a result of rotation around TD [3-8]. Also the experimental results of the lattice rotations of cube-oriented f.c.c. single crystals during plane strain compression up to true strains of 1 or 1.5 obtained by A k e f and D r i v e r



[3], Wert et al. [5], Liu et al. [6, 8] and Basson and Driver [7] have shown that different regions of the crystals rotate in opposite senses mainly about TD. This leads to splitting of the original crystal into complementary texture components. From the point of view of the active slip systems, this rotation results from the operation of one of two pairs of slip systems, and leads to rotations about  $\langle 100 \rangle \parallel \text{TD}$ . Obviously, this rotation leads to major changes in the matrix orientation (towards the hard  $\{110\}\langle 011 \rangle$  orientation) and which are often observed. The present work shows the same behaviour at strains of less than about 1 (see for example figure 3). At higher strains, which are nominally about 1 but, for the cube crystallite may well be about 2 because of the very heterogeneous material flow in this crystal, the local orientations are new starting points for deformation band formation. Figure 7b shows that in the advanced stages of band development single slip systems may be activated (without necessarily participating in the initial matrix re-orientation). This situation could result from the operation of a single slip system of  $\{111\}\langle 110 \rangle$ -type, for which one of the  $\langle 112 \rangle$ -type vectors, the rotation axis, lies on the slip plane and is also perpendicular to the slip direction. The angular vicinity of the  $\langle 112 \rangle$  and  $\langle 111 \rangle$  vectors produces a relative stabilization of the latter in the process of strain localization within the bands. Depending on the selection of the active slip plane in some cases the occurrence of particular external axis/axes in the rotation process can be expected.

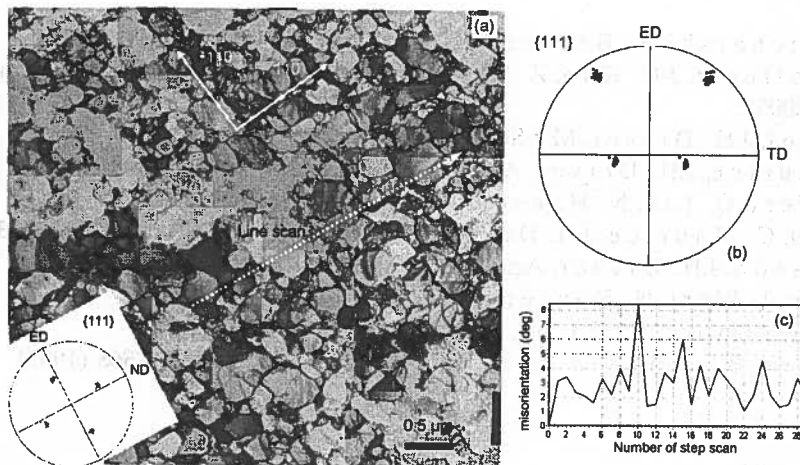


Fig. 7. (a) TEM cell microstructure in a crystallite with 'hard' orientation, and (b) the corresponding  $\{111\}$  pole figure. (c) Misorientation along line scan along ND, with respect to the first measured point. TEM/CBED measurements. Sample deformed 59%

The microstructure observed in TEM (Fig. 7) inside the crystallite with 'hard' orientation, is composed of nearly equiaxed cells with a diameter of  $0.3\text{-}0.5\mu\text{m}$ . Observation in the ND-ED section shows that this substructure is formed as a result of the operation of two pairs of slip systems. From a crystallographic point of view it is characterised by a relatively small orientation spread identified along a line scan

parallel to ND. The misorientation angle formed between the particular sub-cells only sporadically exceeds  $10^\circ$ .

#### 4. Conclusions

The bicrystal deformation analysis shows that the microtexture evolution in each crystallite is quite different. Very strong deformation banding in the 'cube' grain is initiated by strain incompatibilities and gives an initial rotation about the TD. At very high strains where the flow is inhomogeneous  $\langle 112 \rangle$ -type rotations are seen, suggesting a single  $\{111\}\langle 110 \rangle$ -type slip system active in the band. The 'hard'  $\{110\}\langle 011 \rangle$ -oriented grains are more stable under plane strain conditions and tend to develop a nearly uniform dislocation substructure. The incompatibilities resulting from the changes of the shape in both grains influence the formation of the transition zone in the 'hard'-oriented crystallite. This region, with strong disturbances of the crystal lattice, could be a privileged site for new grain nucleation in recrystallization even at room temperature.

#### REFERENCES

- [1] M. Blicharski R. Becker, H. Hu, *Acta metall mater.* **41**, 2007 (1993).
- [2] S. Zaefferer, J-C. Kuo, Z. Zhao, M. Winning, D. Raabe, *Acta mater.* **51**, 4719 (2003).
- [3] A. Akef, J.H. Driver, *Mat Sci Engn.* **A132-245** (1991).
- [4] C. Maurice, J.H. Driver, *Acta metall mater.* **41-1653** (1993).
- [5] J.A. Wert, Q. Liu, N. Hansen, *Acta mater.* **45:2565** (1997).
- [6] Q. Liu, C. Maurice, J.H. Driver, N. Hansen, *Metall Trans.* **29A:2333** (1998).
- [7] F. Basson, J.H. Driver, *Acta mater.* **48:2101** (2000).
- [8] Q. Liu, J. Wert, N. Hansen, *Acta mater.* **48:4267** (2000).
- [9] I.L. Dillamore, H. Kato, *Metal Sci.* **8:73** (1974).
- [10] C.S. Lee, B.J. Duggan, R.E. Smallman, *Acta metall.* **41:2565** (1993).

Received: 24 January 2005.